How to cite: *Angew. Chem. Int. Ed.* **2023**, *62*, e202303561
doi.org/10.1002/anie.202303561

Metal Phosphonate MOFs

Targeted Synthesis of a Highly Stable Aluminium Phosphonate Metal–Organic Framework Showing Reversible HCl Adsorption

Timm M. Reichenau[+], Felix Steinke[+], Michael T. Wharmby, Christian Näther, Tobias A. Engesser, and Norbert Stock**

Abstract: A concept for obtaining isoreticular compounds with tri- instead of tetravalent metal cations using highly acidic reaction conditions was developed and successfully applied in a high throughput study using N,N′-piperazinebis(methylenephosphonic acid) (H_4PMP), that resulted in the discovery of a new porous aluminium phosphonate denoted CAU-60·6 HCl. The high-throughput study was subsequently extended to other trivalent metal ions. Al-CAU-60·6 HCl demonstrates reversible desorption of HCl (18.3 wt % loading) with three distinct compositions observed with zero, four or six HCl molecules per formula unit. Structural changes were followed in detail by powder X-ray diffraction, EDX analysis as well as IR spectroscopy. Rapid desorption of HCl in water within minutes and subsequent adsorption from the gas phase and from aqueous solution are shown. Furthermore, it is possible to adsorb HBr into the guest free Al-CAU-60 framework, demonstrating the high stability of this compound.

Introduction

Porous coordination networks (PCNs), also known as metal organic frameworks (MOFs),[1] have attracted immense interest in the scientific community due to their modular composition, which allows tuning of their pore size and pore surface properties.[2] The progress achieved within the last 25 years was recently summarized and impressively demonstrates the outstanding properties that can be achieved, particularly in adsorption related applications.[3] For example, specific MOFs have been discovered that show exceptional uptake or selectivity towards gases and vapours such as C_2H_2,[4] CH_4,[5] CO,[6] CO_2,[7] SO_2,[8] NO_2[9] or H_2S.[10] Adsorption of the latter adsorbates is especially challenging, as it requires MOFs with exceptionally high chemical stability. Those formed from tri- and tetravalent metal ions such as Al^{3+}, Cr^{3+}, Ti^{4+} or Zr^{4+}, have proven particularly suitable for such selective adsorptions. For example a systematic study of eleven MOFs was undertaken to investigate their use for H_2/HCl separation,[11] an important step in the purification of syngas in the refinery industry,[12] which is currently performed using non-regenerable adsorbents (Table S1.1). Only two of the frameworks, i.e. Zr-UiO-66 and Cr-MIL-101 could reversibly adsorb HCl; molecular dynamic simulation allowed identification of metal centres as the adsorption sites.[11] Functional groups such as amino groups are also suitable to reversibly bind acids and Cr-MIL-101-NH_2, the amino functionalised version of Cr-MIL-101, has been successfully employed.[13] Other MOFs are reported to show HCl uptake, though this results in destruction of the MOF or irreversible chemisorption.[11,14]

Metal phosphonates, a less well-studied subgroup of MOFs, are known to be chemically stable, in particular in combination with tri- and tetravalent metal ions, due to the higher charge of the phosphonate compared to the carboxylate group.[15,16] Aluminium is of special interest due to its high charge-to-radius ratio ($r(Al^{3+}) = 53.5$ pm),[17] its high abundance[18] and its low toxicity.[19] Nevertheless, only six porous aluminium phosphonates are known (Table S2.1)[20,21] N,N′-piperazinebis(methylene-phosphonic acid) (H_4PMP) is one of the most thoroughly studied phosphonate linkers (Figure S2.2) since it is easily synthesized in a one step process from cheap starting materials.[22] Although most of the compounds exhibit dense structures, there are also porous ones such as STA-12 ($[M_2(H_2O)_2(PMP)]\cdot x\,H_2O$, M = divalent ion),[23] or MIL-91 ($[M^{III}/Ti^{IV}(OH_n)(H_2PMP)]\cdot x\,H_2O$, $n=1$ for M^{3+}, $n=0$ for Ti^{4+}) which exhibits a remarkably high sorption capacity for CO_2.[21,24,25] Charge balance in the isoreticular MIL-91 compounds (Al^{3+} vs Ti^{4+}) is accomplished through deprotonation of μ-OH groups of the Inorganic Building Unit (IBU). Similar examples have been reported in the chemistry of metal carboxylates, for example with CAU-1 and MIL-125 containing Al^{3+} and Ti^{4+} ions, respectively.[26] The potentially porous compound $[Zr_2H_4(PMP)_3]\cdot 9\,H_2O$ has a framework which may be protonated at either the IBU or the linker.[27] Like MIL-91, this variable framework protonation would allow exchange of the tetravalent Zr^{4+} ions for trivalent

[*] T. M. Reichenau,[+] F. Steinke,[+] Dr. M. T. Wharmby, Prof. Dr. C. Näther, Dr. T. A. Engesser, Prof. Dr. N. Stock
Institute of Inorganic Chemistry, Christian-Albrechts-University Kiel
Max-Eyth-Str. 2, 24118 Kiel (Germany)
E-mail: stock@ac.uni-kiel.de
Prof. Dr. N. Stock
Kiel Nano, Surface and Interface Science KiNSIS, Christian-Albrechts-Universität zu Kiel
Christian-Albrechts-Platz 4, 24118 Kiel (Germany)
[+] These authors contributed equally to this work

Al^{3+} to yield an isoreticular compound (Figure 1). Protonation of all framework components might be achieved by using highly acidic syntheses conditions.

Results and Discussion

The high-throughput (HT) investigation of the system $AlCl_3$/H_4PMP/NaOH/HCl focused on the parameter space with a large excess of HCl in order to ensure protonation of the linker. The molar ratio Al^{3+} to H_4PMP ratio was varied between 1:0.5 and 1:2 while the molar ratio Al^{3+} to NaOH was varied between 1:2.5 and 1:0 and the molar ratio Al^{3+} to HCl between 1:0 and 1:30. The studied parameter space and the synthesis results are shown in Figure 2.

In our experiment, well-known Al-MIL-91[21,24] is only observed when NaOH was added. Increasing the amount of HCl in the reaction mixture resulted in the formation of two highly crystalline phases, $[Al_2H_{10}(PMP)_3]Cl_4{\cdot}4\,H_2O$ and $[Al_2H_{12}(PMP)_3]Cl_6{\cdot}6\,H_2O$, which are denoted Al-CAU-60·6 HCl and Al-CAU-60·4 HCl, respectively. Thus product formation mainly depends on the molar ratio of Al^{3+} to HCl, while the molar ratio of Al^{3+} to H_4PMP plays a minor role. Single crystals of Al-CAU-60·6 HCl were obtained by extending the reaction time from 36 to 84 hours and increasing the reaction temperature from 160 to 180 °C. By contrast, Al-CAU-60·4 HCl could only be synthesized as a microcrystalline powder. An in-depth description of the HT investigation including exact amounts of starting materials and reaction conditions leading to single crystals of Al-CAU-60·6 HCl is provided in the section 3 of the Supporting Information.

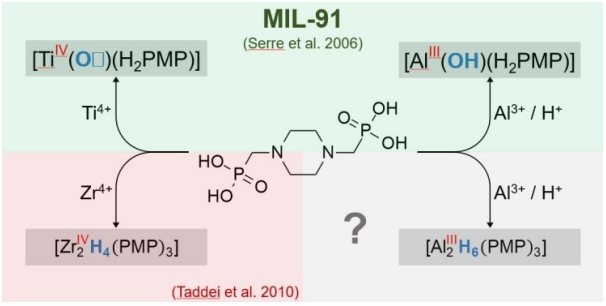

Figure 1. Schematic representation of the synthesis concept derived from observations on MIL-91, which can be obtained employing Ti^{4+} or Al^{3+}. To balance the lower charge of Al^{3+}, an additional proton is introduced into the MIL-91 framework.[21] In $[Zr_2H_4(PMP)_3]$, four protons are scrambled across three linker molecules.[27] However, it should be theoretically possible to introduce additional protons into the framework by protonating the linker. This should open the possibility to synthesize an isoreticular compound employing Al^{3+} salts.

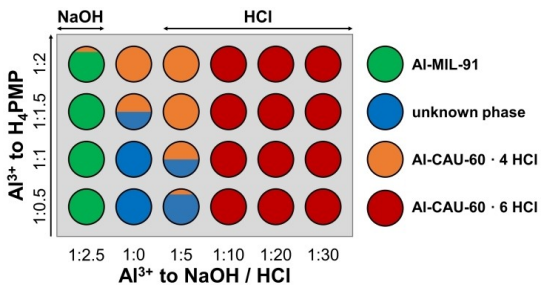

Figure 2. Discovery library and results of the high-throughput (HT) investigation of the system $AlCl_3$ / H_4PMP / NaOH / HCl / H_2O, varying the molar ratio of Al^{3+} to NaOH / HCl (left to right) as well as the molar ratio of Al^{3+} to H_4PMP (top to bottom). Reactions were carried out at 160 °C.

The general applicability of our method is demonstrated in a metal-salt screening HT experiment (Figure S4.5). This resulted in eight isostructural compounds. The framework is formed with trivalent metal ions with ionic radii ranging from 62 (Ga^{3+}) to 91.2 pm (Dy^{3+}). For Ce^{3+} and La^{3+} a new phase of composition $[M_2Cl_4(H_2O)_2(H_2PMP)]$ (M = Ce, La) is found at high HCl concentration (sections S4.3, S5.2 and S6.3).

The structures of Al-CAU-60·6 HCl and Al-CAU-60·4 HCl were determined from single crystal and powder X-ray diffraction (SCXRD and PXRD) data, respectively.[28] Crystallographic data is summarized in Tables S5.1 to S5.4. The asymmetric unit of Al-CAU-60·6 HCl (Fig. S6.1) consists of half a zwitterionic H_4PMP linker molecule, two symmetry independent Al^{3+} ions, a chloride ion and a water molecule. The IBU is composed of octahedrally coordinated Al^{3+} ions that are bridged by phosphonate groups to form chains along the [001] direction. Each IBU is linked to six other IBUs through zwitterionic H_4PMP linker molecules (Figure 3), in which the phosphonate groups are singly protonated and the tertiary amine groups of the piperazine rings are also protonated. The resulting framework is positively charged and has the composition $[Al_2H_{12}(PMP)_3]^{6+}$. Charge balance is accomplished by six Cl^- ions per formula unit, located in the pores. The Cl^- ions form hydrogen bonds with the $-CPO_3H^-$ group and water molecules, which in turn form hydrogen bonds with the protonated piperazine rings (Table S6.1).

The composition $[Al_2H_{12}(PMP)_3]Cl_6{\cdot}6\,H_2O$ corresponds to 18.3 wt % HCl or a concentration of 8.96 mol L^{-1} based on the volume of the unit cell, thus falling within the range of the most effective, reversible HCl MOF adsorbents (Supporting Information, Table S1.1 and S1.2). The structure can be alternatively understood as a neutral framework with six chemisorbed HCl molecules: $[Al_2H_6(PMP)_3]{\cdot}6\,HCl$. Al-CAU-60·6 HCl is therefore clearly isoreticular with the previously reported zirconium phosphonate $[Zr_2H_4(PMP)_3]{\cdot}9\,H_2O$.[27]

The results of the structure refinement of Al-CAU-60·4 HCl show a tilting of one of the three symmetry independent linker molecules (Figure 3e; final Rietveld plot shown in Figure S5.3). The partial desorption of HCl leads to a rearrangement of Cl^- ions and H_2O molecules resulting in the formation of POH···Cl and NH···Cl hydrogen bonds. It must be noted, however, that as the structure is obtained from PXRD data, the protonation state of the functional groups cannot be definitively established and this interpretation is based only on H-bond donor-acceptor distances (Table S6.2, Figure S6.2).

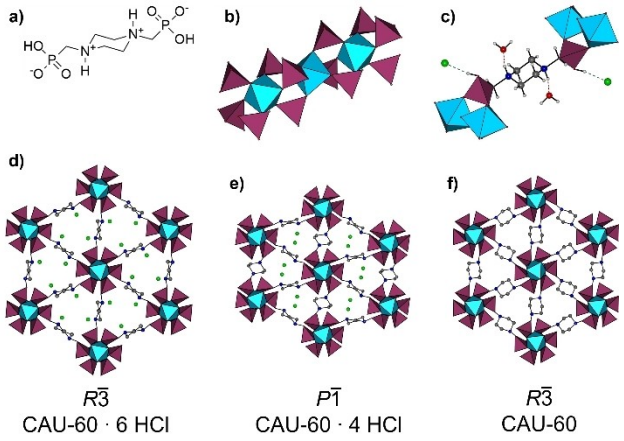

Figure 3. Structural representations of Al-CAU-60, bearing the **wnf** network topology (see Supporting Information, section S6.2), with differing HCl loading grades. a) Zwitterionic linker as found in the fully HCl-loaded Al-CAU-60·6 HCl. b) Rod-shaped IBU composed of octahedrally surrounded Al^{3+} ions that are bridged by phosphonate groups. c) Surrounding of the H_4PMP linker as present in Al-CAU-60·6 HCl. Hydrogen bonds (dashed bonds) are formed between the protonated piperazine moiety and water guest molecules. The protonated P-OH groups form hydrogen bonds to the chloride guest ions (d) Framework structure of Al-CAU-60·6 HCl along [001] with Cl^- ions in the pores. Each IBU is connected by six H_4PMP linkers to six other IBUs. e) Framework structure of Al-CAU-60·4 HCl along [100] with Cl^- ions in the pores. Two out of the six linkers are tilted. f) Framework structure of the HCl free Al-CAU-60 along [001]. All linkers are tilted. Aluminium in light blue, oxygen in red, phosphorous in purple, carbon in grey, nitrogen in dark blue, chlorine in green. Water molecules are omitted for clarity.

The observation that CAU-60 exists in different protonation states prompted us to carry out systematic HCl desorption experiments. Immersing Al-CAU-60·6 HCl in deionized water results in the rapid release of HCl [Figure S7.2, Eq. (1)] within 2 minutes, which is accompanied by a drastic change in pH from 7 to 2 and an increase of conductivity of the solution.

$$[Al_2(H_4PMP)_3]Cl_{6(s)} + 6\ H_2O_{(l)} \rightleftharpoons [Al_2(H_2PMP)_3]_{(s)} + 6\ H_3O^+_{aq} + 6\ Cl^-_{aq} \quad (1)$$

Stability tests of CAU-60·6 HCl and for comparison for Ni-STA-12, Al-MIL-91, $[Zr_2H_4(PMP)_3]\cdot 9H_2O$ in aqueous solutions of varying pH values were carried out to demonstrate the high stability of CAU-60. Details can be found in the Supporting Information section 8. PXRD data show that the stability of the metal phosphonates depends not only on the valency of the metal, but also on the crystal structure. For example, Ni-STA-12 is stable in the most basic media tested (pH 13) whereas for $[Zr_2H_4(PMP)_3]\cdot 9H_2O$ structural break down is only indicated by broad reflections of low intensity. Similarly Al-MIL-91 is fully dissolved under highly acidic media, whilst CAU-60 is stable. The data also shows that at pH 13 for the same structure type, the Zr analogue is more stable than the Al one.

To quantitatively understand the HCl desorption processes that take place during the HCl desorption, an Al-CAU-60·6 HCl dispersion in HCl solution (2 mol L^{-1}) was titrated against NaOH ($c = 1$ mol L^{-1}) and samples were isolated and characterized at well-defined pH values by PXRD and energy dispersive X-ray (EDX) analysis (Figure 4, Supporting Information section 7). The first clear structural change takes place around pH 2.25: new reflections are observed in the PXRD pattern, in addition to those of the starting compound, which can be assigned to a phase with reduced HCl loading. This phase is not Al-CAU-60·4 HCl but a compound crystallizing in the space group *R*-3, which according to EDX data, contains fewer than six HCl molecules per formula unit. Further NaOH was added and it was observed that the two phases co-exist up to pH 3. Above pH 3 shifts of the diffraction peaks of the second phase indicate the occurrence of gradual structural changes due to HCl desorption, further emphasizing the flexibility of the network. At pH 6, a Cl^- free phase was obtained, denoted Al-CAU-60. Some Na^+ and Cl^- residues could be detected in this sample by EDX analysis, but these could be removed by washing with deionized water. The structure of HCl free Al-CAU-60 was elucidated from PXRD data using Rietveld refinement (Figure S.5.2). The structure exhibits features of both the six HCl parent compound and CAU-60·4 HCl: the linker molecules are all tilted so that the plane of the ring is perpendicular to the channel direction (Figure 3e); this allows the structure to crystalize in the higher symmetry space group *R*-3. Interestingly, CAU-60·4 HCl was not observed by PXRD during the titration experiment; we attribute this to the non-equilibrium conditions and diffusion processes in the crystals.

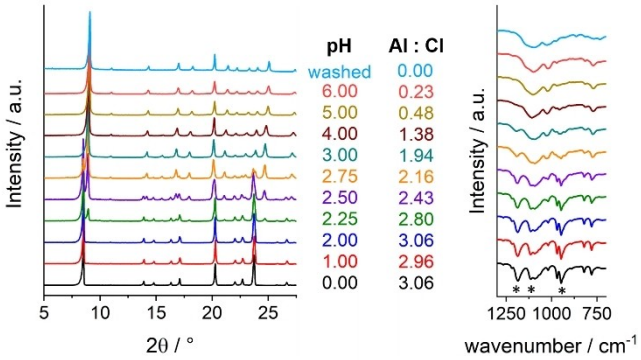

Figure 4. PXRD patterns (left) and IR spectra (right) of samples taken at different pH values when desorbing HCl from Al-CAU-60·6 HCl by addition of NaOH. The PXRD data suggest that the phase transformation occurs in the range of pH 2 to pH 3. This is followed by further slight structural changes in the range of pH 3 to 6. Within the IR spectra, a disappearance of the P–O stretching bands associated with the phosphonate group POH (1186, 1115 and 949 cm^{-1}, marked with asterisks) can be observed with increasing pH value. The Al to Cl ratio obtained by EDX measurements should be interpreted as a qualitative trend due to the high margin of error for EDX measurements. The complete PXRD patterns are shown in Figure S7.2, the complete IR spectra are presented in Figure S8.5.

Full reversibility of the HCl desorption was demonstrated by exposing the HCl-free Al-CAU-60 to aqueous HCl ($c \geq 1$ mol L^{-1}). The incorporation of HBr from solution ($c \geq 2$ mol L^{-1}) is also possible and leads to the formation of Al-CAU-60·6 HBr (section S7.4). The pores of Al-CAU-60 are also accessible to HCl gas, which was produced by reacting NaCl with concentrated H_2SO_4. The gas was passed through 50 mg of a sample in a glass tube for one hour. PXRD and EDX data are shown in Figure S7.6 and Table S7.2, respectively, and confirm the reversible uptake. Similar to $[Zr_2H_4(PMP)_3]\cdot 9\,H_2O$, none of the CAU-60 compounds are porous to N_2. We attribute this observation to the flexibility of the framework, as previously asserted by Taddei et al.[27]

In situ and ex situ IR spectroscopy measurements were carried out to further elucidate the HCl desorption process (Figure 4 right, Figure S9.4 and Table S9.1). DRIFTS measurements allowed us to identify bands associated with H_2O molecules, which facilitated the assignment of the other vibrational bands involving H atoms (Figure S9.1–S9.3). For Al-CAU-60·6 HCl no evidence of amine hydrochlorides is found, confirming the results of the SCXRD measurement where Cl^- ions form hydrogen bonds with the P-OH group. Ex situ IR spectra of samples isolated at different pH-values during the titration experiment are shown in Figure 4 (right), full details are given in section S9. The decrease of intensity of the PO–H stretching vibration is clearly visible, which indicates that deprotonation takes place on the $-PO_3H^-$ group. This observation is also in line with the higher acidity of phosphonic acids in comparison to quaternary ammonium groups. The pK_{a2} value of methylphosphonic acid ($pK_{a2} = 7.29$)[29] is, for example, smaller than that of the trimethylammonium ion ($pK_a = 9.80$).[30]

The existence of the partially and fully protonated framework of Al-CAU-60 prompted us to also study the HCl uptake of $[Zr_2H_4(PMP)_3]\cdot 9\,H_2O$. Stirring of a sample for 24 h in an HCl solution (2 mol L^{-1}) led to the formation of $[Zr_2H_8(PMP)_3]Cl_4\cdot x\,H_2O$ in concentrated HCl (36.7 wt %) (Supporting Information section S7.5).

Conclusion

To conclude, the proposed synthesis concept of using highly acidic conditions to synthesize isoreticular MOFs containing tri- instead of tetravalent metal ions, whereby charge balance is achieved by protonation of the framework, was successfully applied. Moreover, due to the highly acidic conditions compounds with higher degrees of protonation than necessary for charge balance of the framework alone were obtained. Furthermore, this synthetic approach is transferable to a large range of trivalent metal ions. Reversible desorption of HCl takes place in aqueous solution and adsorption is also possible from the gas phase. Protonation of the phosphonate group during HCl adsorption was confirmed by SCXRD and IR spectroscopy. In addition to HCl, HBr is also adsorbed and HCl adsorption could also be demonstrated with the isoreticular Zr compound.

Acknowledgements

Financial support by the state of Schleswig-Holstein is acknowledged. We thank Erik Svensson Grape for his support in the topological analysis of CAU-60 and Marvin Radke for the help during the revision of the manuscript. Open Access funding enabled and organized by Projekt DEAL.

Conflict of Interest

The authors declare no conflict of interest.

Data Availability Statement

The data that support the findings of this study are available in the Supporting Information of this article.

Keywords: Aluminium Phosphonate · Framework Stability · HCl Adsorption · High-Throughput · Metal–Organic Framework

[1] A. Schneemann, V. Bon, I. Schwedler, I. Senkovska, S. Kaskel, R. A. Fischer, *Chem. Soc. Rev.* **2014**, *43*, 6062–6096.
[2] a) H.-C. Zhou, J. R. Long, O. M. Yaghi, *Chem. Rev.* **2012**, *112*, 673–674; b) K. J. Gagnon, H. P. Perry, A. Clearfield, *Chem. Rev.* **2012**, *112*, 1034–1054; c) H. Furukawa, K. E. Cordova, M. O'Keeffe, O. M. Yaghi, *Science* **2013**, *341*, 1230444; d) H.-C. J. Zhou, S. Kitagawa, *Chem. Soc. Rev.* **2014**, *43*, 5415–5418; e) A. Kirchon, L. Feng, H. F. Drake, E. A. Joseph, H.-C. Zhou, *Chem. Soc. Rev.* **2018**, *47*, 8611–8638; f) O. M. Yaghi, *J. Am. Chem. Soc.* **2016**, *138*, 15507–15509.
[3] R. Freund, S. Canossa, S. M. Cohen, W. Yan, H. Deng, V. Guillerm, M. Eddaoudi, D. G. Madden, D. Fairen-Jimenez, H. Lyu, L. K. Macreadie, Z. Ji, Y. Zhang, B. Wang, F. Haase, C. Wöll, O. Zaremba, J. Andreo, S. Wuttke, C. S. Diercks, *Angew. Chem. Int. Ed.* **2021**, *60*, 23946–23974.
[4] a) M. O. Barsukova, K. A. Kovalenko, A. S. Nizovtsev, A. A. Sapianik, D. G. Samsonenko, D. N. Dybtsev, V. P. Fedin, *Inorg. Chem.* **2021**, *60*, 2996–3005; b) S.-Q. Yang, F.-Z. Sun, P. Liu, L. Li, R. Krishna, Y.-H. Zhang, Q. Li, L. Zhou, T.-L. Hu, *ACS Appl. Mater. Interfaces* **2021**, *13*, 962–969.
[5] a) D. Saha, Z. Bao, F. Jia, S. Deng, *Environ. Sci. Technol.* **2010**, *44*, 1820–1826; b) L. Kong, R. Zou, W. Bi, R. Zhong, W. Mu, J. Liu, R. P. S. Han, R. Zou, *J. Mater. Chem. A* **2014**, *2*, 17771–17778; c) X. Wang, Y. Wang, K. Lu, W. Jiang, F. Dai, *Chin. Chem. Lett.* **2021**, *32*, 1169–1172.
[6] K.-J. Ko, H. Kim, Y.-H. Cho, H. Lee, K.-M. Kim, C.-H. Lee, *J. Chem. Eng. Data* **2022**, *67*, 1599–1616.
[7] a) J. An, S. J. Geib, N. L. Rosi, *J. Am. Chem. Soc.* **2010**, *132*, 38–39; b) J. J. Gassensmith, H. Furukawa, R. A. Smaldone, R. S. Forgan, Y. Y. Botros, O. M. Yaghi, J. F. Stoddart, *J. Am. Chem. Soc.* **2011**, *133*, 15312–15315; c) Y. Zhu, Y.-M. Wang, S.-Y. Zhao, P. Liu, C. Wei, Y.-L. Wu, C.-K. Xia, J.-M. Xie, *Inorg. Chem.* **2014**, *53*, 7692–7699.
[8] a) M. R. Tchalala, P. M. Bhatt, K. N. Chappanda, S. R. Tavares, K. Adil, Y. Belmabkhout, A. Shkurenko, A. Cadiau, N. Heymans, G. de Weireld, G. Maurin, K. N. Salama, M. Eddaoudi, *Nat. Commun.* **2019**, *10*, 1328; b) Y. L. Fan, H. P. Zhang, M. J. Yin, R. Krishna, X. F. Feng, L. Wang, M. B. Luo, F. Luo, *Inorg. Chem.* **2021**, *60*, 4–8; c) W. Zhang, W. Jia, J. Qin,

L. Chen, Y. Ran, R. Krishna, L. Wang, F. Luo, *Inorg. Chem.* **2022**, *61*, 11879–11885.
[9] L. J. Small, S. E. Henkelis, D. X. Rademacher, M. E. Schindelholz, J. L. Krumhansl, D. J. Vogel, T. M. Nenoff, *Adv. Funct. Mater.* **2020**, *30*, 2006598.
[10] a) P. M. Bhatt, Y. Belmabkhout, A. H. Assen, Ł. J. Weseliński, H. Jiang, A. Cadiau, D.-X. Xue, M. Eddaoudi, *Chem. Eng. J.* **2017**, *324*, 392–396; b) Y. Belmabkhout, P. M. Bhatt, K. Adil, R. S. Pillai, A. Cadiau, A. Shkurenko, G. Maurin, G. Liu, W. J. Koros, M. Eddaoudi, *Nat. Energy* **2018**, *3*, 1059–1066; c) E. Martínez-Ahumada, A. López-Olvera, V. Jancik, J. E. Sánchez-Bautista, E. González-Zamora, V. Martis, D. R. Williams, I. A. Ibarra, *Organometallics* **2020**, *39*, 883–915.
[11] J. Liu, W. Xia, W. Mu, P. Li, Y. Zhao, R. Zou, *J. Mater. Chem. A* **2015**, *3*, 5275–5279.
[12] a) H. L. Fleming, K. P. Goodboy, E. K. Saforo, US4762537A, **1987**; b) C. C. Chao, US5688479A, **1996**; c) M.-T. Lee, Z.-Q. Wang, J.-R. Chang, *Ind. Eng. Chem. Res.* **2003**, *42*, 6166–6170.
[13] N. Gargiulo, A. Peluso, P. Aprea, L. Micoli, A. Ausiello, M. Turco, O. Marino, R. Cioffi, E. Jannelli, D. Caputo, *ACS Appl. Mater. Interfaces* **2018**, *10*, 14271–14275.
[14] R. Sharma, J. Cousin-Saint-Remi, S. Tiriana, M.-P. Delplancke, S. Pletincx, K. Baert, T. Hauffman, H. Terryn, G. V. Baron, J. F. M. Denayer, *Int. J. Hydrogen Energy* **2022**, *47*, 20556–20560.
[15] G. K. H. Shimizu, R. Vaidhyanathan, J. M. Taylor, *Chem. Soc. Rev.* **2009**, *38*, 1430–1449.
[16] a) T. Devic, C. Serre, *Chem. Soc. Rev.* **2014**, *43*, 6097–6115; b) T. Rhauderwiek, H. Zhao, P. Hirschle, M. Döblinger, B. Bueken, H. Reinsch, D. de Vos, S. Wuttke, U. Kolb, N. Stock, *Chem. Sci.* **2018**, *9*, 5467–5478; c) S. J. I. Shearan, N. Stock, F. Emmerling, J. Demel, P. A. Wright, K. D. Demadis, M. Vassaki, F. Costantino, R. Vivani, S. Sallard, I. Ruiz Salcedo, A. Cabeza, M. Taddei, *Crystals* **2019**, *9*, 270.
[17] R. D. Shannon, *Acta Crystallogr. Sect. A* **1976**, *32*, 751–767.
[18] F. Cardarelli, *Materials handbook. A concise desktop reference*, Springer, London, **2008**.
[19] a) K. Klotz, W. Weistenhöfer, F. Neff, A. Hartwig, C. van Thriel, H. Drexler, *Dtsch. Arztebl. Int.* **2017**, *114*, 653–659; b) Agency for Toxic Substances and Disease Registry, "Public health statement on the toxicological profile of aluminum", **2008**.
[20] a) K. Maeda, J. Akimoto, Y. Kiyozumi, F. Mizukami, *Angew. Chem. Int. Ed. Engl.* **1995**, *34*, 1199–1201; b) K. Maeda, J. Akimoto, Y. Kiyozumi, F. Mizukami, *J. Chem. Soc. Chem. Commun.* **1995**, *19*, 1033–1034; c) S.-F. Tang, J.-J. Cai, L.-J. Li, X.-X. Lv, C. Wang, X.-B. Zhao, *Dalton Trans.* **2014**, *43*, 5970–5973; d) T. L. Kinnibrugh, V. I. Bakhmutov, A. Clearfield, *Cryst. Growth Des.* **2014**, *14*, 4976–4984; e) F. Steinke, A. Javed, S. Wöhlbrandt, M. Tiemann, N. Stock, *Dalton Trans.* **2021**, *50*, 13572–13579.
[21] C. Serre, J. A. Groves, P. Lightfoot, A. M. Z. Slawin, P. A. Wright, N. Stock, T. Bein, M. Haouas, F. Taulelle, G. Férey, *Chem. Mater.* **2006**, *18*, 1451–1457.
[22] D. Villemin, B. Moreau, A. Elbilali, M.-A. Didi, M.'h. Kaid, P.-A. Jaffrès, *Phosphorus Sulfur Silicon Relat. Elem.* **2010**, *185*, 2511–2519.
[23] a) J. A. Groves, S. R. Miller, S. J. Warrender, C. Mellot-Draznieks, P. Lightfoot, P. A. Wright, *Chem. Commun.* **2006**, 3305–3307; b) M. T. Wharmby, G. M. Pearce, J. P. S. Mowat, J. M. Griffin, S. E. Ashbrook, P. A. Wright, L.-H. Schilling, A. Lieb, N. Stock, S. Chavan, S. Bordiga, E. Garcia, G. D. Pirngruber, M. Vreeke, L. Gora, *Microporous Mesoporous Mater.* **2012**, *157*, 3–17.
[24] N. Hermer, M. T. Wharmby, N. Stock, *Z. Anorg. Allg. Chem.* **2017**, *643*, 137–140.
[25] P. L. Llewellyn, M. Garcia-Rates, L. Gaberová, S. R. Miller, T. Devic, J.-C. Lavalley, S. Bourrelly, E. Bloch, Y. Filinchuk, P. A. Wright, C. Serre, A. Vimont, G. Maurin, *J. Phys. Chem. C* **2015**, *119*, 4208–4216.
[26] a) T. Ahnfeldt, N. Guillou, D. Gunzelmann, I. Margiolaki, T. Loiseau, G. Férey, J. Senker, N. Stock, *Angew. Chem. Int. Ed.* **2009**, *48*, 5163–5166; b) M. Dan-Hardi, C. Serre, T. Frot, L. Rozes, G. Maurin, C. Sanchez, G. Férey, *J. Am. Chem. Soc.* **2009**, *131*, 10857–10859.
[27] M. Taddei, F. Costantino, R. Vivani, *Inorg. Chem.* **2010**, *49*, 9664–9670.
[28] Deposition Numbers 2225671 (for Al-CAU-60), 2225672 (for Al-CAU-60·4HCl), 2225673 (for Al-CAU-60·6HCl), 2225674 (for Dy-CAU60·6HCl), 2225675 (for Fe-CAU-60·6HCl), 2225676 (for Ga-CAU-60·6HCl), 2225677 (for Lu-CAU-60·6HCl), 2225678 (for Sc-CAU-60·6HCl), 2225679 (for V-CAU-60·6HCl), 2225680 (for Yb-CAU-60·6HCl), 2225681 (for Y-CAU-60·6HCl) and 2225682 (for $[La_2Cl_4(H_2O)_2(H_2PMP)]$) contain the supplementary crystallographic data for this paper. These data are provided free of charge by the joint Cambridge Crystallographic Data Centre and Fachinformationszentrum Karlsruhe Access Structures service.
[29] E. P. Serjeant, B. Dempsey, *Ionisation constants of organic acids in aqueous solution*, Pergamon, Oxford, **1979**.
[30] M. Abul Kashem Liton, M. Idrish Ali, M. Tanvir Hossain, *Comput. Theor. Chem.* **2012**, *999*, 1–6.

Manuscript received: March 10, 2023
Accepted manuscript online: April 9, 2023
Version of record online: May 17, 2023